ResearchGate

See discussions, stats, and author profiles for this publication at: https://www.researchgate.net/publication/228708014

Monte Carlo Simulations of Small Sulfuric Acid–Water Clusters †

ARTICLE *in* THE JOURNAL OF PHYSICAL CHEMISTRY B · NOVEMBER 2001

Impact Factor: 3.3 · DOI: 10.1021/jp0116499

CITATIONS
36

READS
28

2 AUTHORS:

Shawn M Kathmann
Pacific Northwest National Laboratory
83 PUBLICATIONS **1,099** CITATIONS
SEE PROFILE

Barbara Hale
Missouri University of Science and Technology
54 PUBLICATIONS **635** CITATIONS
SEE PROFILE

Available from: Barbara Hale
Retrieved on: 27 January 2016

Monte Carlo Simulations of Small Sulfuric Acid−Water Clusters†

S. M. Kathmann‡,* and B. N. Hale§,*

Environmental Molecular Sciences Laboratory, Pacific Northwest National Laboratory, Richland, Washington 99353, and Physics Department, University of Missouri−Rolla, Rolla, Missouri 65409

Received: May 1, 2001; In Final Form: August 7, 2001

Effective atom−atom potentials are developed for binary sulfuric acid−water clusters and applied in a Bennett Metropolis Monte Carlo calculation to determine free energy differences for small neighboring sized clusters of fixed composition at 298 K. The atom−atom pair potentials consist of Lennard-Jones short-range and Coulombic long-range terms and assume rigid $SO_4^{2\delta-}$ with two unconstrained $H^{\delta+}$ and rigid H_2O molecules interacting via revised central force (RSL2) potentials. The potential parameters are determined from both ab initio studies and tests of the potential using the statistical mechanical formalism for binary cluster size distributions. In the potential tests, fixed composition free energy differences, $\delta f_{km,m}$, for $[H_2O]_{km}[H_2SO_4]_m$ clusters are plotted versus $(km + m)^{-1/3}$, and the resulting slope and intercept (in the large cluster regime) are used to extract model dependent binary liquid surface tension and partial vapor pressures at 298 K. The potential parameters are adjusted to obtain approximate agreement with experimental surface tension and partial vapor pressures for $k = 1$ and 4 (84% and 57% weight percent H_2SO_4, respectively). The free energy differences for $m \leq 15$ are presented, together with internal cluster energy contributions, snapshots of cluster structure, and evidence for onset of the large cluster regime near $m = 5$. The long-range goals have been to test the free energy difference procedure for studying binary cluster properties and to develop model potentials appropriate for the simulation of small binary clusters at low temperatures characteristic of stratospheric sulfuric acid−water aerosols.

I. Introduction

Small binary clusters of H_2O and H_2SO_4 play a crucial role in atmospheric processes ranging from ordinary vapor-to-liquid nucleation[1−5] to acid rain formation[6−8] and ozone depletion mechanisms.[9−11] Doyle's early work[2] predicted that even in undersaturated atmospheres a sulfuric acid vapor pressure of 10^{-9} Torr can produce binary nucleation with water. The ability of H_2SO_4 to enhance nucleation together with its proposed role in ozone depletion has generated great interest in the formation of $H_2O-H_2SO_4$ clusters. The actual process of cluster formation is further complicated because sulfuric acid dissociates in water. This raises questions regarding the role of neutral ($H_2SO_4 \cdot H_2O$) versus ionic ($HSO_4^- \cdot H_3O^+$) complexes in the kinetics of the clustering reactions prior to the formation of atmospheric aerosol. Recent evidence suggests that low-temperature liquid sulfuric acid clusters absorb nitric acid.[12−14] Once formed, these mixed clusters of $H_2SO_4 \cdot HNO_3 \cdot H_2O$ grow by subsequent adsorption of water and nitric acid vapor monomers. It has been recognized that the resulting ternary aerosols facilitate heterogeneous chlorine activation in polar stratospheric clouds which depletes the ozone directly.[9,15] However, the detailed clustering reactions and ternary composition remain unclear.[16−18] The precise role that sulfuric acid and water clusters play remains an open question.[9,19]

Of the experiments on vapor to liquid binary nucleation of water and sulfuric acid,[20−25] two report absolute nucleation rates and the remainder note conditions for onset. The analyses of the data (most of it taken near 298 K) reflect the difficulties encountered when working with this system. One difficulty is the extremely low partial vapor pressure of sulfuric acid. A second difficulty lies with the assumptions used in classical nucleation theory (CNT). CNT treats small molecular clusters as if they were tiny liquid droplets characterized by a bulk surface tension and liquid number density. Furthermore, the classical binary nucleation rate depends exponentially on σ^3, where σ is the composition dependent binary liquid surface tension for the critical cluster.[2,4,26−35] A 10% error in σ can affect the nucleation rate by as much as 8 orders of magnitude. In many systems of interest, the critical cluster size is of the order of 10−100 molecules, making the use of bulk surface tension suspect. Another concern is that atmospheric binary nucleation often occurs under conditions where surface tension and density data are unavailable. The binary surface tension $H_2SO_4 \cdot H_2O$ displays large compositional gradients implying pronounced surface enrichment effects.[33] Despite these issues, estimating the onset of nucleation with the classical model has met with some success.[25] However, predicting the temperature dependence of the nucleation rate, J, has presented serious difficulties,[23] with the ratio of experimental to theoretical nucleation rates ranging from 10^{-10} to 10^{10}.

The goals of the present work have been to use a statistical mechanical formalism[36] to determine binary cluster size distributions, to extract an effective surface tension for molecular clusters of fixed composition, and to relate a set of such fixed composition data to the energy of formation of an arbitrary binary critical cluster. Part of the difficulty in binary nucleation formalisms is that one must optimize the critical cluster size and composition for each physical data point. (A data point consists of temperature, T, and activities, $a_i = P_i/P_i^o$ where $i = 1$ and 2, P_i is the ambient vapor pressure of species i, and P_i^o is the equilbrium vapor pressure above the pure liquid.) This means

† Part of the special issue "Howard Reiss Festschrift".

* To whom correspondence should be addressed. E-mail: shawn.kathmann@pnl.gov. E-mail: bhale@umr.edu.

‡ Pacific Northwest National Laboratory.

§ University of Missouri−Rolla.

10.1021/jp0116499 CCC: $20.00 © 2001 American Chemical Society
Published on Web 10/03/2001

that for a single experiment one needs a range of information about how the cluster free energy of formation depends on size, n, and cluster composition ($n = n_1 + n_2$, where n_1 and n_2 are the number of molecules of species 1 and 2, respectively). For example, it would be useful, but not sufficient, to know the discrete molecular formation energies for the addition of successive H_2O molecules to a single H_2SO_4 molecule. It is with the desire to determine the composition and size dependent information in some useful way that we have focused our attention on a statistical mechanical formalism for the cluster distribution function, $N_{km,m}$, where km and m are the number of water and sulfuric acid molecules, respectively. This allows the binary cluster composition to be represented by the water to sulfuric acid molecular ratio, $k = km/m$. The goal is to calculate the free energy differences (between the (km, m) and [$k(m - 1)$, $(m - 1)$] clusters) for a series of clusters with k fixed. Finally, we want to show how this information can be used to determine the maximum in the free energy of formation (find km^* and m^*) given the experimental conditions (T, a_1, and a_2). Our intent is to (1) develop simple effective pair potentials for the water−sulfuric acid system which produce an effective small cluster surface tension consistent with the bulk experimental values at $k = 1$ and 4 (a range of composition relevant to stratospheric aerosols), (2) to demonstrate that a Bennett Metropolis Monte Carlo[37] approach can yield neighboring sized free energy differences which are linear in $(km + m)^{-1/3}$ for fixed composition when $km + m$ is sufficiently large, and (3) to indicate how the statistical mechanical formalism predicts a critical cluster size ($(km + m)^*$) and composition (k^*). In this paper, we report the results of our model effective pair potentials and the calculation of free energy differences for two compositions at $T = 298$ K (where reliable experimental data exist for aqueous sulfuric acid surface tension and liquid density). In the course of describing the formalism, we point out that the potentials must reproduce not only the effective large cluster surface tension, $\sigma(k)$, but also the correct partial vapor pressures above the bulk binary solution with molecular ratio, k. The latter feature of the model emerges from the statistical mechanical formalism using a fixed number density for model clusters at fixed k.

The statistical mechanical formalism for binary clusters is described in section II and the atom−atom pair potentials which assume rigid $SO_4^{2\delta-}$ and H_2O structures with two unconstrained $H^{\delta+}$ ions free to bond with either species are described in section III. In determining the parameters for the atom−atom pair potentials, use is made of ab initio studies of small clusters using GAMESS[38] quantum chemistry software and experimental properties of aqueous sulfuric acid mixtures. The free energy difference calculations are described in section IV and results and conclusions are given in sections V and VI.

II. Binary Cluster Statistical Mechanical Formalism

A. Classical Model in Terms of *km* and *m*. Binary clusters with discrete numbers of molecules are denoted by (km, m), where (as described above) km is the number of molecules of species 1 and m is the number of molecules of species 2. The composition of the cluster is determined by k, the molecular ratio, and the overall size by is determined m. To estimate a classical nucleation rate, J, one must know $N_{km,m}/V$, the number concentration of the binary cluster. For comparison, some quantities in the classical binary nucleation model are introduced and cast into the (km, m) cluster notation. In the classical model, $\ln(N_{km,m}/V) = \ln(c_o) - \Delta\Phi(k, m)$, where c_o (defined below) is related to the monomer concentrations and $\Delta\Phi(k, m)$ is the classical free energy of formation of the (km, m) cluster from km monomers of species 1 and m monomers of species 2. To simplify notation, $\Delta\Phi(k, m)$ is divided by k_BT, where k_B is the Boltzmann constant and T is the temperature. Under normal conditions (fixed T and the species' partial vapor pressures, P^1 and P^2) the free energy surface $\Delta\Phi(k, m)$ has a saddle point at the critical cluster size denoted by k^* and m^*.

The kinetics of multicomponent nucleation display a greater degree of complexity than unary systems because of the variety of possible reaction pathways. Previous[4,29,30,32,35,39−43] studies have investigated binary nucleation fluxes both along the thermodynamic minimum free energy path and those that deviate from this path. A feature called "ridge crossing" can appear for fluxes that do not follow the thermodynamic path of steepest descent. In these cases, the cluster flux travels not through the free energy saddle region but instead skirts over an adjoining ridge. The flux may then continue along a path far removed from that of the lowest free energy. Typically, the clusters associated with the flux along the path of minimum free energy have been assumed to have the greatest affect on the nucleation rate. In general, ridge crossing may be important for systems with broad, flat saddle regions accompanied by large differences in their vapor pressure (kinetic forcing). The identification of those clusters most relevant to the nucleation rate is more difficult for systems that display deviations from the minimum free energy path. Thus, in a rigorous calculation of the binary nucleation rate it is necessary to take into account the growth and decay of clusters with respect to both species. However, in many cases, the nucleation flux grows quickly to a steady-state value and the classical steady-state nucleation rate, J, is well approximated by the product of the number concentration of the critical cluster, $N_{km^*,m^*}/V$, and the "nucleation flux" of monomers of both species to the critical cluster, Z_{kinetic}. Of the several models for J, there are some differences in Z_{kinetic}.[35] However, the basic form of the so-called "classical model binary nucleation rate", $J_{\text{classical}}$, is[3,26−28,34,44]

$$J_{\text{classical}} = Z_{\text{kinetic}} \frac{N_{km^*,m^*}}{V} \tag{1}$$

$$= Z_{\text{kinetic}} c_o(k) \exp[-\Delta\Phi^*] \tag{2}$$

where $c_o(k) = (N_{1,0}^{\text{pure}}/V)^{k/k+1}(N_{0,1}^{\text{pure}}/V)^{1/k+1}$ and $N_{1,0}^{\text{pure}}/V$ and $N_{0,1}^{\text{pure}}/V$ are the vapor monomer concentrations above the bulk pure liquid of species 1 and 2, respectively. The $c_o(k)$ has also been a point of some debate, but the form given above (as pointed out by Wilemski and Wyslouzil) is consistent with the law of mass action.[35]

In terms of k and m, the classical model $\Delta\Phi(k, m)$ takes the form[2,5,29,33]

$$\Delta\Phi(k, m) = A(km + m)^{2/3} - km \ln S_1 - m \ln S_2 \tag{3}$$

where $A(km + m)^{2/3} = 4\pi r^2\sigma/(k_BT)$ is the energy required to form the surface of the binary cluster and the supersaturation $S_i = P^i/P^{io}$ and P^{io} is the equilibrium partial vapor pressure of species i over the binary bulk solution at temperature T and composition k. The r and $\sigma(k)$ are the classical radius of the cluster and the bulk liquid solution surface tension. Using the molecular number density in the liquid solution, $\rho_{\text{liq.sol.}}$, to relate r and $(km + m)$, one finds

$$A = [36\pi]^{1/3} \frac{\sigma(k)}{k_BT\rho_{\text{liq.sol.}}^{2/3}} \tag{4}$$

A line of maxima of $\Delta\Phi(k, m)$ can be determined from $(\partial\Delta\Phi/$

$\partial m)_k = 0$ from which one obtains the following expressions:

$$\frac{2}{3}A(km+m)^{-1/3} - \frac{k}{k+1}\ln S_1 - \frac{1}{k+1}\ln S_2 = 0 \quad (5)$$

or

$$km^*(k) + m^*(k) = \left[\frac{2A(k)}{3\ln S(k)}\right]^3 \quad (6)$$

and

$$\Delta\Phi(k, m^*(k)) = \left[\frac{2}{3\sqrt{3}}\frac{A(k)^{3/2}}{\ln S(k)}\right]^2 \quad (7)$$

where $A(k)$ denotes the k dependence of A, $\ln S(k) \equiv k/(k+1)\ln S_1 + 1/(k+1)\ln S_2 = x\ln S_1(x) + (1-x)\ln S_2(x) \equiv \ln S(x)$, and the mole fraction with respect to water is given by $x \equiv km/(km+m) = k/(k+1)$. This is just the form for the free energy of formation at the saddle point, except that one has not yet determined k^*. Wilemski[33,45] has pointed out that in the classical model the critical composition of the bulk region of the cluster, k_b, satisfies the following expression involving the supersaturations, S_1 and S_2, and the partial molecular volume of species i, v_i, (all functions of k_b):

$$\frac{\ln S_1}{\ln S_2} = \frac{v_1}{v_2}; \quad \text{at } k_b = k_b^* \quad (8)$$

The k_b^* is determined by varying k until eq 8 is satisfied. This procedure requires a model for the cluster "bulk" and "surface" molecules, particularly when surface enrichment occurs.

In a statistical mechanical model for small clusters, however, the cluster is defined to be the system containing $km + m = n$ molecules (or atoms), all of which share equally in generating phase space points for the system ensemble. Thus, in the statistical mechanical model, one must determine k^* by locating the saddle point of $\Delta\Phi(k, m(k))$ (that is, where $\Delta\Phi$ in eq 7 is *minimized)*. The latter condition is satisfied when the so-called *scaled supersaturation* of Binder and Stauffer,[30] $\ln S(k)/A(k)^{3/2} \equiv s(k)$, is maximized:

$$s(k^*) = \mathrm{Max}\left[\frac{\ln S(k)}{A(k)^{3/2}}\right] \quad (9)$$

The $k = k^*$ which maximizes the scaled supersaturation thus determines the size of the critical cluster and its energy of formation:

$$\Delta\Phi(k^*, m(k^*)) = \left[\frac{2}{3\sqrt{3}\,s(k^*)}\right]^2 \quad (10)$$

Using this procedure, one can scale the binary critical cluster energy of formation in a manner similar to the unary case.[46,47]

B. Statistical Mechanical Formalism. The statistical mechanical formalism for binary clusters used in the present calculations is based on a formalism developed by Hale and Ward[48] for single component clusters[49,50] and extended to binary systems by Hale and Kathmann.[36] This formalism, which treats the vapor−binary cluster system with the classical grand canonical partition function, is based on the following assumptions. (1) First, it is assumed that the binary vapor system with volume, V, is a mixture of noninteracting ideal gases, with each distinct binary cluster (km, m) constituting an ideal gas system. Thus, one obtains the following expression:[51,52]

$$\frac{N_{km,m}}{(N_{1,0})^{km}(N_{0,1})^m} = \frac{e^{\mu_{km,m}/k_BT}Z_{km,m}}{[e^{\mu_{1,0}/k_BT}Z_{1,0}]^{km}[e^{\mu_{0,1}/k_BT}Z_{0,1}]^m} \quad (11)$$

where $\mu_{km,m}$ and $Z_{km,m}$ are the chemical potential and canonical partition function of the (km, m) cluster. (2) Second, the assumption is made that each ideal gas composed of $N_{km,m}$ clusters is in equilibrium with $N_{1,0}$ and $N_{0,1}$ monomer "clusters" in the vapor−cluster system. That is, for the model water and sulfuric acid binary system

$$km(H_2O) + m(H_2SO_4) \leftrightarrow [(H_2O)_{km}(H_2SO_4)_m] \quad (12)$$

This dynamic equilibrium assumption gives $\mu_{km,m} = km\mu_{1,0} + m\mu_{0,1}$, and thus the chemical potentials cancel in eq 11. (3) The final assumption of the model is that the (km, m) cluster is described by a classical Hamiltonian with three independent configurational and three independent momentum degrees of freedom per atom and an interaction potential, $U = \sum_{ij}U(|\mathbf{r}_i - \mathbf{r}_j|)$, dependent only on position vectors, $\mathbf{r}_i$. For such a system, the integrations over the classical momenta (the classical translational partition functions) cancel in eq 11, and one obtains the following form for $N_{km,m}$ in terms of the (km, m) cluster configurational integral, $Q_{km,m}$:

$$\frac{N_{km,m}}{(N_{1,0})^{km}(N_{0,1})^m} = \frac{Q_{km,m}}{(km)!m!(Q_{1,0})^{km}(Q_{0,1})^m}. \quad (13)$$

After multiplying and dividing the right-hand side of eq 13 by the product $\Pi_{m'=1}^{m'=m-1}Q_{km',m'}$, one can derive the following form for $N_{km,m}$:

$$N_{km,m} = Q_0 \exp\sum_{m'=1}^{m}\{-\delta f_{km',m'} - k\ln I_1 - \ln I_2 + k\ln S_1 + \ln S_2\} \quad (14)$$

where the symbols in eq 14 are defined as follows:

$$I_1 \equiv \left[\frac{N_{1,0}^o V_{km,m}^o}{kmV}\right]^{-1} = \left[\frac{\frac{k}{k+1}\rho_{\mathrm{liq.sol.}}}{N_{1,0}^o/V}\right] \quad (15)$$

$$I_2 \equiv \left[\frac{N_{0,1}^o V_{km,m}^o}{mV}\right]^{-1} = \left[\frac{\frac{1}{k+1}\rho_{\mathrm{liq.sol.}}}{N_{0,1}^o/V}\right] \quad (16)$$

$$C'_{km,m} \equiv \ln\left[\frac{Q_{km,m}}{Q_{k(m-1),m-1}\left(Q_{1,0}\frac{V_{km,m}}{V}\right)^k\left(Q_{0,1}\frac{V_{km,m}}{V}\right)}\right] \quad (17)$$

$$Q_{0,0} \equiv \frac{V}{V_{k,1}} = Q_0 \quad (18)$$

$$-\delta f_{km,m} \equiv C'_{km,m} + \xi_{km} + (k+1)\ln\alpha \quad (19)$$

and

$$\xi_{km} = \ln\left[\frac{(km)^k(k(m-1))!}{(km)!}\right] \quad (20)$$

The $N_{1,0}^\circ(k)/V$ and $N_{0,1}^\circ(k)/V$ are the equilibrium concentrations of monomers above the bulk liquid solution with composition,

k, $S_1(k) \equiv N_{1,0}/N^{\circ}_{1,0}$ and $S_2(k) \equiv N_{0,1}/N^{\circ}_{0,1}$. This formalism has been derived specifically to calculate free energy differences, $-\delta f_{km,m}$, in binary cluster Monte Carlo simulations. The simulation volume for the (km, m) cluster, $V_{km,m}$, is defined by

$$V_{km,m} = V^{o}_{km,m}\alpha = \frac{km + m}{\rho_{\text{liq.sol.}}}\alpha \tag{21}$$

where α is a constant chosen to minimize the effects of cluster boundary conditions. The combinatorial factor, $\xi_{km} \leq 1$ for m larger than five and $\rightarrow 0$ as $m \rightarrow \infty$.

The variation of $\ln(N_{km,m})$ with respect to m holding k fixed is the discrete version of the partial derivative with respect to m:

$$\delta_m \ln(N_{km,m})_k = -\delta f_{km,m} + k \ln S_1 + \ln S_2 - k \ln I_1 - \ln I_2 \tag{22}$$

which is simply the quantity in braces $\{\cdots\}$ in eq 14 evaluated at the upper limit of the sum. It is useful to compare $\delta_m \ln(N_{km,m})_k$ to what one expects in the classical nucleation model, $\partial/\partial m\ [\ln(N_{km,m})_{\text{classical}}]_k = -\partial\Delta\Phi_{km,m}/\partial m|_k$. In making the approximation, $\delta_m \ln N_{km,m} \approx -\partial\Delta\Phi_{km,mk}\partial m|_k$, one obtains an expression which provides some insight into how $-\delta f_{km,m}$ depends on $km + m$ and how one might predict experimental quantities from the calculated free energy differences. That is, one finds (for $S_1 = S_2 = 1$)

$$\frac{-\delta f_{km,m}}{k+1} \approx -\frac{2}{3}A[km + m]^{-1/3} + \frac{k \ln I_1 + \ln I_2}{k+1} \tag{23}$$

Equation 23 is used to analyze the calculated free energy differences. However, this expression is not needed to determine $N_{km,m}/V$ (nor equivalently to calculate the statistical mechanical free energy of formation). In the statistical mechanical model, one simply sums the free energy differences. In any case, it is useful to plot the calculated data for the left-hand side of eq 23 versus $[km + m]^{-1/3}$ for k fixed. If the calculated free energy differences (for fixed k) are well approximated by eq 23, then the data in the large cluster regime should approach a straight line with slope equal to $-{}^2/_3A$ and intercept given by the I_1 and I_2. In the statistical mechanical model, one can show that in the limit as $m \rightarrow \infty$, for fixed k, and $S_1(k) = S_2(k) = 1$, the following condition holds:

$$\frac{-\delta f_{km,m}}{k+1} \rightarrow \frac{k \ln I_1 + \ln I_2}{k+1} \tag{24}$$

One can think of the large cluster $-\delta f_{km,m}$ data (dependent as they are on the model potential parameters) as predicting an effective surface tension (to be compared with the experimental bulk liquid surface tension, $\sigma(k)$) and an extrapolated intercept (to be compared with the experimental values for $\ln I_1(k)$, $\ln I_2(k)$, and $\rho_{\text{liq.sol.}}$). The latter $I_1(k)$ and $I_2(k)$ are determined from the partial vapor pressures and liquid solution density at composition k. In practice, the experimental intercept provides a scale for the magnitude of the calculated $-\delta f_{km,m}$. The intercept is thus related to the chemical potential of the molecules within the clusters. Furthermore, the data for model sulfuric acid−water clusters should fall above the equivalent $C_{km=n}$ data for model water clusters.[50]

The statistical mechanical formalism for $-\delta f_{km,m}$ provides an alternate way of looking at cluster energies of formation. For example, the extremal value of the "free energy of formation" in the statistical mechanical formalism can be found from eq 22 by setting $\delta_{\text{m}} \ln(N_{km,m})_k = 0$:

$$\frac{-\delta f_{km,m}}{k+1} - \frac{k \ln I_1 + \ln I_2}{k+1} + \frac{k \ln S_1 + \ln S_2}{k+1} = 0 \tag{25}$$

from which one can determine the k dependent value of $m^*(k)$. If $k = k^*$ (the critical composition) then $m^*(k^*) = m^*$ and the binary critical cluster size is determined. The task thus returns to the determination of k^*. The rigorous approach calls for using $\delta_k \ln(N_{km,m})_m = 0$ and the calculation of $-\delta f_{km,m}$ for a range of k values. This is a formidable task which we propose can be simplified by noting the relationship between k and the slopes of the $-\delta f_{km,m}/k+1$ versus $(km + m)^{-1/3}$.

In the present work, the $-\delta f_{km,m}$ are calculated for two values of k using a Bennett Metropolis Monte Carlo technique[37,53] and effective atom−atom pair potentials for the interactions described in the next section. Because no dissociative potentials were available for the H_2SO_4−H_2O system, it was necessary to develop the potentials as part of this investigation.

III. H_2SO_4−H_2O Potential Model

Because stratospheric conditions allow for the formation of supercooled sulfuric acid aerosols[54,55] with compositions ranging from 60 to 85 wt % H_2SO_4,[56] the model potentials should be applicable for k ranging from 4 (57%) to 1 (84%). A number of features of the H_2SO_4−H_2O system are relevant to the development of a potential. For example, the chemistry of sulfuric acid−water mixtures is characterized by complicated hydrogen bonding. Further, both sulfuric acid and water possess fairly large polarizabilities and dipole moments (2.72[57] and 1.85 D, respectively). Most important, however, is the question of ionization of the H_2SO_4 in the clusters. Consider the reaction producing an ionic complex, $H_2SO_4 + H_2O \leftrightarrow HSO_4^-{\cdot}H_3O^+$, as opposed to the reaction producing the neutral complex, $H_2SO_4 + H_2O \leftrightarrow H_2SO_4{\cdot}H_2O$. Ab initio results suggest the neutral complex is preferred in the gas phase over the ionic complex.[58] However, the ionic complex becomes more stable as ambient water monomers cluster around the neutral complex.[59] Studies imply there must be rather complicated reaction schemes in order to account for the hydrogen transfer mechanisms between molecules/ions in these small clusters.[60] In reality, each cluster may contain several species: H_2O, H_2SO_4, H_3O^+, HSO_4^-, SO_4^{-2}, $H_5O_2^+$, etc.

To keep the model as simple as possible while incorporating the most prevalent intracluster species into the simulations, the potential model assumes rigid H_2O and $SO_4^{2\delta-}$ (sulfate) molecular structures with $H^{\delta+}$ ions free to bond with either species, as proposed in the preliminary version of the potential.[36] This permits, for example, $H_5O_2^+$ (oxonium), HSO_4^- (bi-sulfate or hydrogen sulfate), and H_3O^+ (hydronium) ions. It also satisfies a requirement of the free energy difference simulation scheme, i.e., that the cluster components must revert automatically to the neutral monomer species when the interactions between H_2O and H_2SO_4 are turned off. The molecular structure of sulfuric acid[61] (where all sulfur−oxygen bonds are tetrahedrally coordinated around the sulfur) is used as a starting point for the SO_4^{-2} geometry (see Figure 1 for details of the $SO_4^{2\delta-}$ structure). The sulfur atom in the sulfuric acid molecule is said to be "hypervalent", thus, allowing the sulfur atom to maintain two S−O single bonds and two S═O double bonds. It is the S−O single bond groups which are bonded to the hydrogen atoms. In the model, this is reflected in two different effective charges for the O atoms in the H_2SO_4 molecule.

It is assumed that the water molecules, sulfate ions, and hydrogen ions in the binary clusters interact through combined

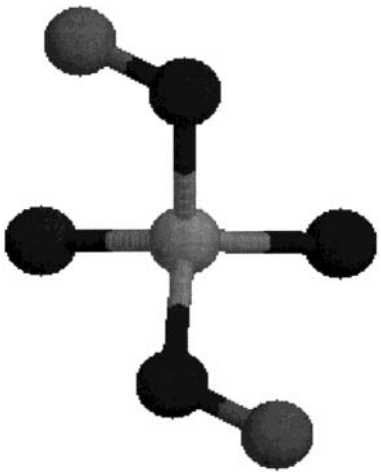

Figure 1. Model used for the structure of the sulfuric acid molecule. The dark spheres are oxygen atoms tetrahedrally bonded to the sulfur atom in the $SO_4^{2\delta-}$, and the undissociated $H^{\delta+}$ atoms are the small gray spheres. The experimental structure parameters are d(S−O) = 1.574 Å, d(S═O) = 1.422 Å, d(O−H) = 0.97 Å, O−S−O angle = 101.3°, O═S═O angle = 123.3°, and S−O−H angle = 108.5°.

Coulomb plus Lennard-Jones effective atom−atom pair potentials given by[36]

$$U = \sum_{i,j} \frac{q_i q_j}{r_{ij}} + \sum_{i,j} 4\epsilon_{ij}\left[\left(\frac{\sigma_{ij}}{r_{ij}}\right)^{12} - \left(\frac{\sigma_{ij}}{r_{ij}}\right)^{6}\right] \qquad (26)$$

r_{ij}, σ_i, ϵ_i, and q_i are the distance between atoms i and j, the Lennard-Jones distance parameter for atom i, the Lennard-Jones well-depth parameter for atom i, and charge for atom i, respectively. For the water−water interactions, the revised central force potentials RSL2[62] are used. The combination rules $\sigma_{ij} = (\sigma_i + \sigma_j)/2$ and $\epsilon_{ij} = \sqrt{\epsilon_i \epsilon_j}$ are assumed in eq 26. The fundamental potential parameters q_i, σ_i, and ϵ_i, have been chosen in part from the results of GAMESS[38] quantum mechanical studies of sulfuric acid and water and in part from empirical studies of sulfuric acid and water as described below.

The relative magnitudes of the Mulliken charges q_i were obtained from quantum chemical calculations using a Gaussian DZV+3P basis set at the restricted Hartree−Fock level of theory.[38] Initially, these relative charges were scaled to match experimental dipole moments. The trial potentials were then used to produce a plot of $-\delta f_{km,m}$ versus $(km + m)^{-1/3}$ for k = 1 and 4 at 298 K. The intent was to extract from the plot a potential model dependent bulk liquid solution surface tension (proportional to the slope) and model dependent partial vapor pressures (from the extrapolated intercept) of the calculated data. The experimental values for the surface tension at T = 298 K for k = 1 and 4 are 68.5 and 76.0 dyn/cm, respectively. The experimental equilibrium partial vapor pressures for sulfuric acid and water at T = 298 K for k = 1 and 4 are $P_{k=1}^{wo} = 3.9 \times 10^{-2}$ Torr and $P_{k=4}^{wo} = 5.0$ Torr (for water) and $P_{k=1}^{ao} = 1.6 \times 10^{-5}$ Torr and $P_{k=4}^{ao} = 1.3 \times 10^{-9}$ Torr (for sulfuric acid). A major complication was the necessity to obtain a realistic dependence on the composition, k. First, the potential parameters (essentially the q_i) were varied in a range that kept the resulting dipole moments for sulfuric acid and water close to their experimental values. It was found that the k = 4 cluster results consistently predicted an intercept that was much larger than the experimental intercept. Next, an attempt was made to include polarization effects by placing a scalar isotropic polarizability on the oxygen site of each water molecule. This increased the computational effort considerably, and the problems associated with the compositional dependence not only persisted but were amplified. Thus, (having produced no improvement in the potential and making the search less tractable) the polarization terms were dropped. The procedure thus became one of varying the potential parameters without restricting the charges to yield experimental dipole moments but still keeping the species neutral. The goal was to obtain approximate agreement with experimental bulk liquid solution surface tension (for both k values in the large cluster regime) and to obtain extrapolated intercepts which were consistent with experimental partial vapor pressures. This involved simulating clusters as large as km = 60 water molecules and m = 15 acid molecules for k = 4. The final potential parameters which produce reasonable agreement with experimental surface tension and partial vapor pressures at 298 K are given in Table 1 for sulfuric acid and water.

TABLE 1: Potential Parameters for H_2SO_4−H_2O where q_i is the Charge for Atom i, σ_i is the Lennard-Jones Distance Parameter for Atom i, and ϵ_i is the Lennard-Jones Well-Depth Parameter for Atom i[a]

atom	q_i (|e|)	σ_i (Å)	ϵ_i (kcal/mol)
S_a	0.4000	3.0	1.5
O_{a1}	−0.1621	2.2	0.2
O_{a2}	−0.2007	2.4	0.2
H_a	0.1627	1.8	0.4
O_w	−0.1315	2.0	0.8
H_w	0.0657	1.8	0.2

[a] S_a is the sulfur atom, O_{a1} and O_{a2} are the single and double bonded oxygen atoms, respectively, and H_a are the hydrogen atoms of the sulfuric acid molecule. O_w is the oxygen atom, and H_w are the hydrogen atoms of the water molecule.

IV. Cluster Free Energy Differences

The Bennett Metropolis Monte Carlo technique[37] provides a convenient method of calculating the configurational free-energy difference, $\Phi_B - \Phi_A = -\ln(Q_B/Q_A)$, between two systems, A and B, with differing interaction potentials. In the present calculations, the free energy differences, $C'_{km,m} \equiv \ln[Q_B/Q_A]$, are given by eq 17. Thus, A and B refer to cluster systems A and B each containing km molecules of species 1 and m molecules of species 2. The interaction potentials in the two systems differ as follows. In the B ensemble, all molecules (and their constituent atoms) interact normally. In the A ensemble, the interactions of k "probe" molecules of species 1 (water) and a *single* "probe" molecule of species 2 (sulfuric acid) with the rest of the cluster are "turned off" so that the probe molecules behave like $k + 1$ free molecules in the simulation volume, $V_{km,m}$ (see Figure 2). In this way, the B ensemble models the (km, m) cluster and the A ensemble models the ($k(m - 1)$,($m - 1$)) cluster and $k + 1$ free monomers in the volume, $V_{km,m}$. A practical approach is to reduce the interactions of the probes with all other molecules by a factor, $\lambda \ll 1$. In the limit as $\lambda \rightarrow 0$, the free energy differences approach the physical descriptions given above, and the configurational partition function for the A ensemble becomes $Q_A = Q_{k(m-1),(m-1)}(Q_{1,0})^k(Q_{0,1})$. The total potential energy U_A of the A ensemble is written in terms of λ as follows:

$$U_A = \sum_{i,j} u_{ij} + \lambda \sum_{k,l} u_{kl} \qquad (27)$$

where u_{ij} is the interaction potential between the ith and jth atom and the first summation is over all fully interacting atoms. The second summation includes only those interactions in which atoms of the probe molecules (denoted by index l) interact with

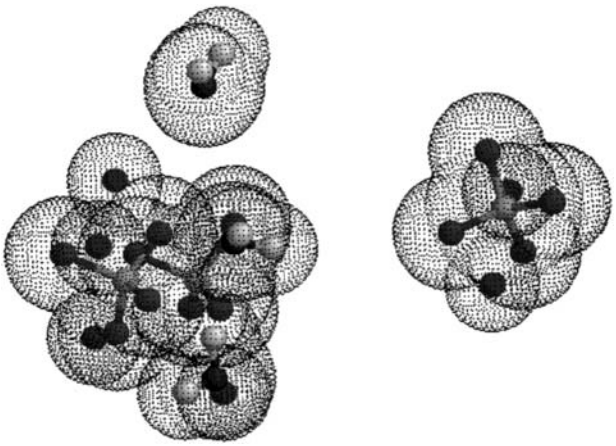

Figure 2. Snapshot of an A cluster containing three sulfuric acid molecules and three water molecules. The probes are one sulfuric acid molecule and one water molecule. See Figure 1 for atom assignment.

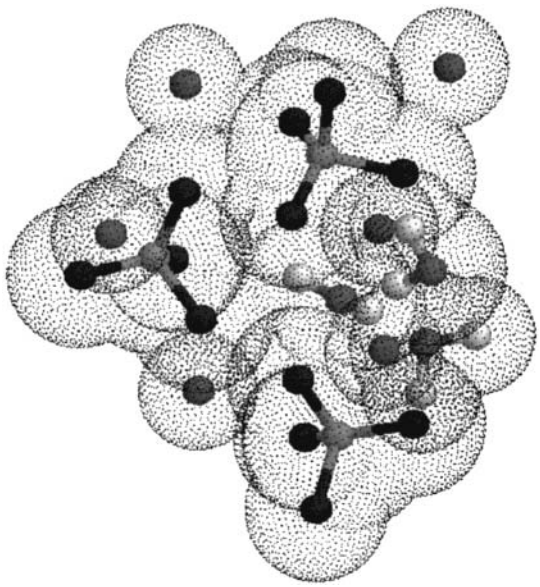

Figure 3. Snapshot of a B cluster containing three sulfuric acid molecules and three water molecules. All molecules interact normally. See Figure 1 for atom assignment.

atoms of nonprobe molecules or with atoms of *other* probe molecules. Atoms within the same probe molecule (such as the H^+ and atoms of SO_4^{-2} in H_2SO_4) are not reduced by λ. For the B ensemble, all molecules interact fully (see Figure 3), so that $Q_B = Q_{km,m}$ and

$$U_B = \sum_{i,j} u_{ij} + \sum_{k,l} u_{kl} \tag{28}$$

In Bennett's technique, $Q_B/Q_A = \langle f(\Delta U - C)\rangle_A/\langle f(-\Delta U - C)\rangle e^C$, where the Fermi function, $f(x) = (1 + e^x)^{-1}$, and $\langle f\rangle_{A(B)}$ indicate a Metropolis Monte Carlo average of the Fermi function f over ensemble A(B). The *functional form* for ΔU is as follows $\Delta U \equiv U_B - U_A = (1 - \lambda)\sum_{k,l} u_{kl}$ and is evaluated in each system during the Monte Carlo runs. The $\langle f\rangle_{A(B)}$ are calculated for a range of C values chosen to bracket the $C = C'_{km,m}$ value for which $\langle f\rangle_A/\langle f\rangle_B = 1$. When the latter condition is satisfied, one obtains $C'_{km,m} = \ln (Q_B/Q_A)$.

As described in section III, using eq 23, one can extract an approximate "effective binary surface tension", $\sigma(k)$, for the binary clusters from the slope of $-\delta f_{km,m}/[k + 1]$ providing all of the $-\delta f_{km,m}$ have the same composition, k, and all of the model cluster densities approach the same $\rho_{liq.sol.}$ as $m \rightarrow \infty$. It is for this reason the $-\delta f_{km,m}$ are calculated for a range of m values at fixed k and for cluster simulation volumes having the same number density. To examine "effective cluster surface tension" at another composition, k, one must repeat the Monte Carlo simulations for a range of m values at a different simulation volume number density.

The Metropolis Monte Carlo technique[53,63] is used to calculate canonical ensemble averages of the model clusters. For this purpose, a cluster of sulfuric acid and water is defined as $km + m$ molecules confined to move within a spherical volume, $V_{km,m}$, (see eq 21) which is α times larger than the bulk liquid volume $\rho_{liq.sol.}^{-1}$ of solution[64] for an equivalent number of molecules. In the present work, we set $\alpha = 5$. Lee et al.[65] noted that the Helmholtz free energy for small Lennard-Jones argon clusters is relatively insensitive to the simulation radius, r_{sim}, for $\alpha \approx 5$. Some studies of the dependence on α were made for small water cluster free energy differences[66] and for a few small (km, m) clusters. It was found that α ranging from 5 to 7 produces values of $-\delta f_{km,m}$ within the normal uncertainty range. The latter uncertainty is (in these calculations) about ± 0.5 for $-\delta f_{km,m}/(k + 1)$. The initial molecular configurations were chosen at random using an algorithm which performed random molecular translations and rotations until all of the molecules fit within the simulation volume $V_{km,m}$ and every atom was at least a specified distance (2 Å) from atoms in another molecule.

At each Monte Carlo step during the simulation, random displacements (and rotations) are generated for all rigid units (H_2O, $SO_4^{2\delta-}$, and $H^{\delta+}$) simultaneously. If this results in the placement of any atom outside the constraining volume, the process is repeated until all atoms are within $V_{km,m}$. Random translations occur simultaneously along three mutually orthogonal directions ($\hat{x}$, $\hat{y}$, $\hat{z}$), and random rotations are made about one of the axes chosen at random. The maximal displacement is of the order of $d_{max} = 0.04$ Å, and the maximal rotation is about $\beta_{max} = 0.06$ rad. The value used for the free energy parameter is $\lambda = 10^{-5}$.

A probe set ($k + 1$ probe molecules) must be chosen for both A and B ensembles and consists of k water molecules plus one sulfuric acid molecule. In the A ensemble, the probe set is uniquely determined by those atoms whose interactions are reduced by λ. In the B ensemble, however, any set of k water molecules plus one sulfuric acid molecule serves as a probe set. One can greatly increase the efficiency of determining $\langle f(-\Delta U - C)\rangle_B$ by averaging $f(-\Delta U - C)$ over multiple probe sets. In the interest of maintaining manageable run times, the present calculations made averages over m^2 probe sets (for $k = 1$) for the smaller clusters. For larger clusters and for $k = 4$, up to 40 probe sets were included. Some of the calculations for $m > 10$ included 120 probe sets.

In generating the free energy differences, it is necessary to make several runs for each cluster, starting from different initial configurations. A tractable approach is to equilibrate the B ensemble cluster and then create an A ensemble cluster from the final B configuration. Additional starting configurations can be generated by switching the A and B cluster configurations, by adding molecules to smaller clusters, or by heating the cluster then quenching to the simulation temperature. One must also monitor the ΔU in each ensemble as its distribution is a means of monitoring the sampling process. As a secondary monitor, the average cluster potential energy divided by m (the number of acid molecules) is plotted versus m. From this plot, one can detect unequilibrated clusters and other anomalous cluster states, which generally are related to trapping in potential energy wells.

TABLE 2: Comparison of Cluster Free Energy Differences, $-\delta f_{km,m}$, and Average B Ensemble, Cluster Interaction Energies for $k = 1$[a]

m	$-\delta f_{km,m}/k+1$	U_B	U_{aa}	U_{aw}	U_{ww}	steps (M)
1	2.7	−13	0	−3	0	5
2	8.0	−38	−27	−8	−3	10
3	10.6	−68	−44	−15	−8	10
4	12.0	−101	−62	−24	−14	15
5	14.4	−141	−81	−36	−24	15
6	15.8	−178	−102	−45	−31	15
7	15.9	−214	−123	−56	−35	15
8	16.1	−253	−148	−69	−37	15
9	16.0	−290	−166	−78	−46	10
10	16.5	−334	−189	−89	−57	16
15	17.1	−521	−308	−138	−77	10
20	17.6 ± 1.0	−714	−427	−197	−91	9

[a] U_B, U_{aa}, U_{aw}, and U are the total acid−acid potential energies, acid−water potential energies, and water-water potential energies, respectively. All interaction energies are in kcal/mole. MC steps denotes the total number of Monte Carlo steps (in million) required to achieve equilibrium and to calculate the $-\delta f_{km,m}$. m is the number of sulfuric acid molecules and $T = 298$ K.

TABLE 3: Comparison of Cluster Free Energy Differences, $-\delta f_{km,m}$, and Average B Ensemble, Cluster Interaction Energies for $k = 4$[a]

m	$\delta_m F/k+1$	U_B	U_{aa}	U_{aw}	U_{ww}	steps (M)
1	5.3	−34	0	−10	−14	10
2	10.5	−96	−24	−30	−42	15
3	12.4	−163	−39	−53	−70	15
4	14.0	−231	−55	−78	−98	15
5	14.9	−309	−72	−108	−130	15
7	14.9	−432	−115	−155	−163	15
10	14.8	−692	−151	−251	−290	15
15	15.8	−980	−265	−362	−353	10

[a] U_B, U_{aa}, U_{aw}, and U are the total acid−acid potential energies, acid−water potential energies, and water-water potential energies, respectively. All interaction energies are in kcal/mole. MC steps denotes the total number of Monte Carlo steps (in million) required to achieve equilibrium and to calculate the $-\delta f_{km,m}$. m is the number of sulfuric acid molecules and $T = 298$ K.

About two million Monte Carlo steps are required for the smaller cluster equilibrations. For the larger clusters (and depending on the starting configuration), longer runs of 6−10 million were used. Two independent Bennett Metropolis Monte Carlo computer codes were generated for simulating the (km, m) clusters, and all of the free energy differences, $-\delta f_{km,m}$, were determined from both codes and checked for consistency.

V. Simulation Results

The calculated values of the free energy differences, $-\delta f_{km,m}$, for the model binary sulfuric acid clusters at 298 K for two compositions, $k = 1$ and 4, (corresponding to 84 and 57 wt % sulfuric acid, respectively) are shown in Tables 2 and 3. The cluster sizes simulated are $m = 1-10$ and 15. Some preliminary results are available for $m = 20$. The plots of the model sulfuric acid−water cluster free energy differences are shown in Figures 4 and 5, together with the classical model experimental predictions (dashed lines). Tables 2 and 3 also summarize other average quantities for the clusters calculated during the Monte Carlo simulations.

Before discussing the results, it is noted again that the goal of this study has been to develop effective water−sulfuric acid atom−atom interaction potentials appropriate for simulating small binary clusters of H_2O and H_2SO_4. The specific procedure has been to require that the model Lennard-Jones plus Coulomb atom−atom pair potentials produce (at 298 K and at two compositions, $k = 1$ and 4) cluster free energy differences,

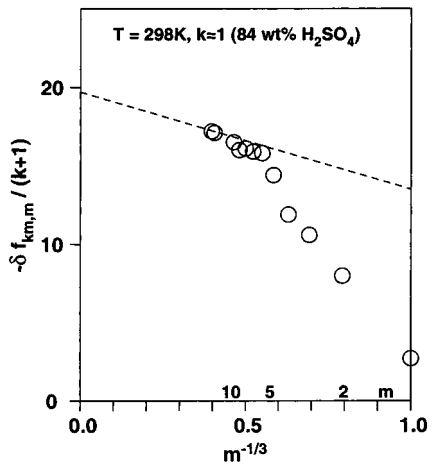

Figure 4. Plot of $-\delta f_{km,m}/[k + 1]$ vs $m^{-1/3}$ for $k = 1$ (84 wt. % H_2SO_4) at $T = 298$ K. $-\delta f_{km,m}$ is the free energy difference between the (km, m) cluster and the [$k(m - 1)$,$(m - 1)$] cluster plus $k + 1$ monomers where km and m are the number of water and sulfuric acid molecules, respectively. The dashed line (- - -) indicates the predicted values from experimental surface tension (68.5 dyn/cm) and partial vapor pressures (3.9×10^{-2} and 1.6×10^{-5} Torr for water and sulfuric acid, respectively) for composition $k = 1$.

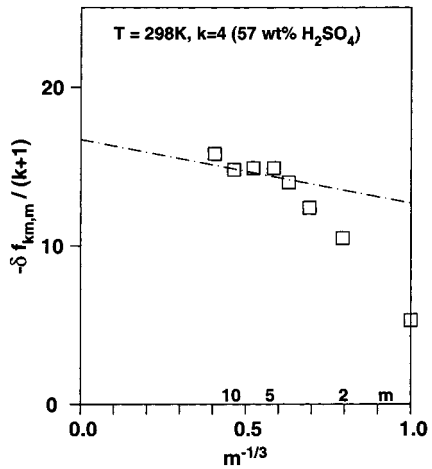

Figure 5. Plot of $-\delta f_{km,m}/[k + 1]$ vs $m^{-1/3}$ for $k = 4$ (57 wt. % H_2SO_4) at $T = 298$ K. $-\delta f_{km,m}$ is the free energy difference between the (km, m) cluster and the [$k(m - 1)$,$(m - 1)$] cluster plus $k + 1$ monomers where km and m are the number of water and sulfuric acid molecules, respectively. The dashed line (- - -) indicates the predicted values from experimental surface tension (76.0 dyn/cm) and partial vapor pressures (5.0 and1.3×10^{-9} Torr for water and sulfuric acid, respectively) for composition $k = 4$.

$-\delta f_{km,m}$, whose large cluster slope versus $(km + m)^{-1/3}$ agree approximately with experimental bulk liquid solution surface tension and whose extrapolated intercept (as $m \rightarrow \infty$) is consistent with the experimental partial vapor pressures. The intercept is proportional to the overall magnitude of the free energy differences, and the slope is proportional to the surface tension. The results in Figures 4 and 5 thus represent the degree to which the effective atom−atom potentials model the binary clusters with varying composition and size and remain consistent with the experimental binary surface tension and partial vapor pressures of water and sulfuric acid at 298 K. The intent is to use these potentials to describe cluster systems at lower temperatures, 190−240 K, characteristic of stratospheric conditions and over a range of compositions, k. In binary nucleation problems, it is essential that a viable microscopic model account accurately for the compositional dependence of the cluster energy of formation.

The plots of $-\delta f_{km,m}/[k+1]$ versus $m^{-1/3}$ show that the model potentials give free energy differences which rise rapidly for $m = 1-5$ and then begin to level out. The total number of molecules in the clusters at $m = 5$ are $km + m = 10$ and $km + m = 25$ for $k = 1$ and 4, respectively. It appears to be within this size range (10 molecules) that most clusters begin to display "bulk" properties associated with the slope and intercept analysis described above. A similar result was found for small model RSL2 water clusters and for model argon Lennard-Jones clusters[50] and for TIP4P water clusters.[67] For $m \geq 5$, the slopes in Figures 4 and 5 display reasonable agreement with the experimental bulk surface tension prediction (dashed lines). One of the major problems in developing the potential model is obtaining consistent k, or composition dependence. When $-\delta f_{km,m}$ is divided by $(k + 1)$, the free energy differences approximate a "per probe molecule" value. Despite this "scaling" in k, obtaining a good k dependence (agreement with the experimental intercepts) requires a careful balance of the acid−acid and acid−water interaction strengths. The calculated data in Figures 4 and 5 indicate that the model potentials produce $-\delta f_{km,m}$ which are consistent with the magnitude of the partial vapor pressures. [It is noted that an order of magnitude uncertainty in the extrapolated experimental sulfuric acid partial vapor pressures due to the low partial vapor pressure of sulfuric acid[68] produces intercept uncertainties of ± 1.3 (± 0.5) for $k = 1$ (4)].

The plots in Figures 4 and 5 show that as the size of the clusters increases ($m \rightarrow \infty$) the smaller k value ($k = 1$) clusters have (on a per probe molecule basis) larger values of $-\delta f_{km,m}/[k+1]$. This is consistent with a lower vapor pressure for pure sulfuric acid compared to the larger vapor pressure for pure water. Any model potential capable of describing small water−sulfuric acid clusters should reproduce this behavior. Similarly, if the results of calculations such as these are to predict binary cluster energies of formation (and nucleation rates) the "effective surface tension" composition or k dependence must be adequately modeled. In these respects, the results shown in Figures 4 and 5 for the model potentials appear to have passed a modest requirement. Future developments of the potential are certainly in order, particularly with respect to incorporation of accurate ab initio cluster energetics, structures, hydrogen motion, and charge distributions.

Experimentally it has been shown that as H_2O is added to pure bulk H_2SO_4 the surface tension increases.[69] In standard liquid solution analysis, this implies that the H_2O resides primarily in the bulk of the mixture rather than at the surface.[70] Furthermore, the temperature dependence of the measured surface tension of sulfuric acid−water solutions indicates that the excess surface entropy per molecule is lower than the excess surface entropy per molecule for pure water.[70,71] This seems plausible considering the extensive hydrogen bonding and strong chemical affinity H_2SO_4 has for H_2O. In Figures 4 and 5, note that $-\delta f_{km,m}$ has been scaled with $1/(k+1)$ so that the slope of the $k = 4$ data is smaller than that for $k = 1$.

Snapshots of the $(km, m) = (8, 2)$ and $(20, 5)$ clusters at 298 K indicate that both the hydrogen ions and the hydrogen atoms from water molecules form hydrogen bonds between water molecules and sulfate ions. The sulfate's oxygen atoms also appear to bond with other sulfur atoms. The simulated model clusters display morphology which suggests that water molecules tend to form rings through the centers of which sulfate ions hydrogen bond to one another. The water rings appear to vary in number and shape with six-membered rings occurring most often.

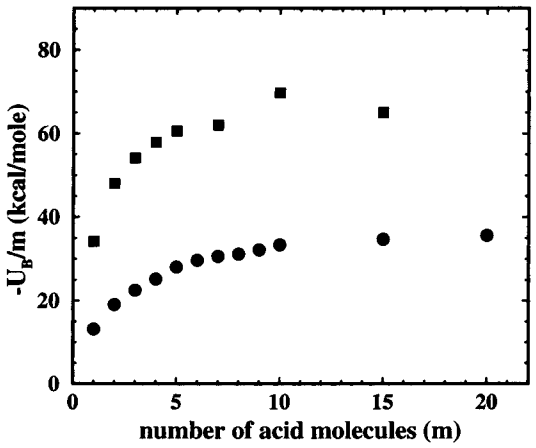

Figure 6. Comparison of the Monte Carlo averages of the total cluster potential energy of the B ensemble per sulfuric acid molecule, $-U_B/m$, versus the number of sulfuric acid molecules, m, for $k = 1$ and 4 at $T = 298$ K. The filled circles and squares denote the $k = 1$ and 4 clusters, respectively.

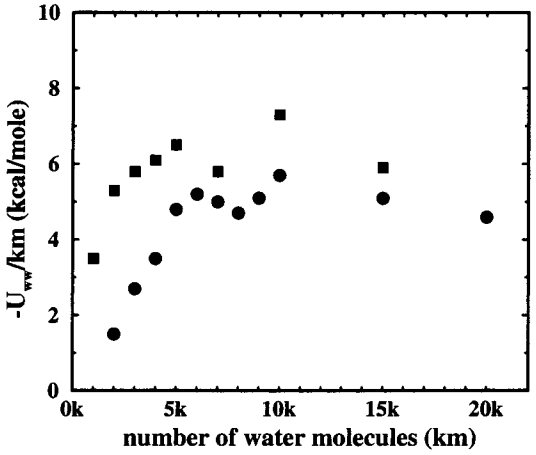

Figure 7. Comparison of the Monte Carlo averages of the water−water potential energy of the B ensemble per water molecule, $-U_{ww}/km$, versus the number of water molecules, km, for $k = 1$ and 4 at $T = 298$ K. The filled circles and squares denote the $k = 1$ and 4 clusters, respectively.

The relative root-mean-square displacements of the ions and molecules indicate that $H^{\delta+}$ ions have a greater mobility than either H_2O or $SO_4^{2\delta-}$. The hydrogen ions in this model appear to interact with many neighbors and can, in some cases, diffuse away from their "parent" sulfuric acid molecules. To determine whether clusters described with this potential model exhibit size effects and surface enrichment/deficiency at larger sizes, further study with larger clusters at various compositions and temperatures will be necessary.

Figures 6 and 7 indicate the behavior of the average total potential energy, U_B, and the water−water interaction potential energy, U_{ww}, in the B cluster, where all of the km water molecules and m sulfuric acid molecules are interacting fully. These calculated potential energies, together with the acid−acid, U_{aa}, and acid−water, U_{aw}, are given in Tables 2 and 3. In Figure 6, the total potential energy (divided by m) versus m indicates the monotonic increase in total energy as m increases for $k = 1$. For $k = 4$, there appears to be some scatter in the $-U_B/m$ values when $m > 5$. This could be a cluster size effect but might result from limited sampling of configurations in the larger clusters. The plot of $-U_{ww}/km$ in Figure 7 shows distinct m dependent variations in the water−water binding for $k = 1$. This is surprising because the total potential energy for $k = 1$

showed no evidence of these oscillations. The same oscillatory behavior appears in the $k = 4$ water−water interaction energy. A speculation is that these oscillations are associated with six-membered ring structure of the water. Note that the $k = 4$ clusters contain 35, 50, and 75 molecules for $m = 7$, 10, and 15, respectively. This corresponds to 133, 190, and 285 atoms, respectively, in each cluster. The larger clusters require longer Monte Carlo runs and appear to be less liquidlike than smaller clusters, suggesting that larger clusters tend to become trapped in energy wells. Many of these clusters were simulated in multiple runs starting from different initial configurations. It is interesting to speculate whether the total potential energy in such model clusters can be smoothed out naturally at the expense of switching potential energy between water−water, acid−water, and acid−acid bonds. If this is the case, the free energy differences have a greater probability of being well behaved and reflecting fewer structural and surface enrichment anomalies.

In the present molecular model, it is of interest to see whether the neutral or ionic complex of sulfuric acid monohydrate is preferred. Simulation results show that the neutral complex is allowed. In this case, the water's oxygen atom is directed toward the sulfuric acid's hydrogen atom. However, with two or more water molecules, the model appears to allow dissociation. The mobility of the $H^{\delta+}$ ions in this model can result in the formation of hydrogen bonds between the water molecules and the sulfate ion(s). Another feature of the model cluster morphology is an apparent "linking" of several water rings to provide a "web" in which the sulfate and hydrogen ions are embedded. The linking of these water rings leaves "channels" through which the sulfate anions are hydrogen bonded to one another down the center of the ring channel. Further simulations should provide information regarding the stability, compositional-dependent structure, and size-dependent structure of these clusters.

VI. Conclusions

This work has presented a molecular simulation of small sulfuric acid−water binary clusters using effective atom−atom potentials which were developed and calibrated at 298 K to yield approximate agreement with the experimental bulk solution surface tension and partial vapor pressures. A special feature of the potential model is the flexibility of hydrogen ion transfer within the clusters. The potential model has been developed within the framework of a statistical mechanical formalism for binary clusters which allows one to calculate free energy differences between neighboring sized clusters with the same mole fraction. These free energy differences, which were calculated for series of small clusters at two mole fractions can be used to determine binary cluster free energies of formation and to predict binary cluster size distributions. As an example, using eqs 14−20 and results of the present calculations for $k = 1$, one can estimate the concentration of (1, 1) water−sulfuric acid dimer clusters at 298 K and a relative humidity of 50%. Assuming a concentration of sulfuric acid monomers, $N_{0,1}/V = 10^{11}$ cm^{-3}:

$$\frac{N_{1,1}}{V} = \rho_{\text{liq.sol.}} \exp\left[-\delta f_{1,1} - \ln\frac{0.5\rho_{\text{liq.sol.}}}{\frac{N_{1,0}}{V}} - \ln\frac{0.5\rho_{\text{liq.sol.}}}{\frac{N_{0,1}}{V}} - \ln 2\alpha\right] \approx 4 \times 10^{8}\ \text{cm}^{-3}$$

The latter concentration can be compared to the prediction of the concentration of water dimers (at the same relative humidity) from the simulations on model RSL2 water clusters, $\approx 10^{13}$ cm^{-3}.[50] It is with such estimates at lower temperatures (190−240 K) in mind that the binary statistical mechanical formalism for free energy differences and the model water−sulfuric acid potentials have been developed. The approach provides a general framework which can be applied to other small binary systems such as nitric acid and water.

Acknowledgment. This work was supported in part by the National Science Foundation Grant No. 93-07318. The preparation of this manuscript was performed in part using the Molecular Science Computing Facility (MSCF) in the William R. Wiley Environmental Molecular Sciences Laboratory a national scientific user facility sponsored by the Department of Energy's Office of Biological and Environmental Research and located at Pacific Northwest National Laboratory. Pacific Northwest National Laboratory is operated for the Department of Energy by Battelle.

References and Notes

(1) Heist, R. H.; Reiss, H. *J. Chem. Phys.* **1974**, *61*, 573.
(2) Doyle, G. J. *J. Chem. Phys.* **1961**, *35*, 795.
(3) Mirabel, P.; Katz, J. L. *J. Chem. Phys.* **1974**, *60*, 1138.
(4) Kiang, C. S.; Stauffer, D. *Faraday Symp. Chem. Soc.* **1973**, *1*, 26.
(5) Laaksonen, A.; Talanquer, V.; Oxtoby, D. *Annu. Rev. Phys. Chem.* **1995**, *46*, 489.
(6) Charlson, R. J. *J. Geophys. Res.* **1983**, *88*, 1375.
(7) Mohnen, V. A. *Sci. Am.* **1988**, *259*, 14.
(8) Hedin, L. O.; Likens, G. E. *Sci. Am.* **1996**, *275*, 88.
(9) Peter, T.; Carslaw, K. S.; Clegg, S. L. *Reviews of Geophysics*, **1997**, *35*, 125.
(10) Tolbert, M. A. *Science* **1996**, *272*, 1597.
(11) Ravishankara, A. R.; Hanson, D. R. *J. Geophys. Res.* **1996**, *101*, 3885.
(12) Carslaw, K. S. *Geophys. Res. Lett.* **1994**, *21*, 2479.
(13) Tabazadeh, A.; Turco, R. P.; Jacobson, M. Z. *J. Geophys. Res.* **1994**, *99*, 12897.
(14) Tabazadeh, A.; Turco, R. P.; Drdla, K., Jacobson, M. Z.; Toon, O. B. *Geophys. Res. Lett.* **1994**, *21*, 1619.
(15) Hanson, D. R.; Ravishankara, A. R. *J. Geophys. Res.* **1991**, *96*, 17307.
(16) Solomon, S. *Rev. Geophys.* **1988**, *26*, 131.
(17) Solomon, S.; Garcia, R. R.; Rowland, F. S.; Wuebbles, D. J. *Nature* **1986**, *321*, 755.
(18) Solomon, S.; Garcia, R. R.; Ravishankara, A. R. *J. Geophys. Res.* **1994**, *99*, 20491.
(19) *Scientific Assessment of Ozone Depletion*: World Meteorological Organization, 1991; Rep. 25.
(20) Reiss, H.; Margolese, D. I.; Schelling, F. J. *J. Colloid Interface Sci.* **1976**, *56*, 511.
(21) Bouland, D.; Madelaine, G.; Vigla, D.; Bricard, J. *J. Chem. Phys.* **1977**, *66*, 4854.
(22) Mirabel, P.; Clavelin, J. *J. Chem. Phys.* **1978**, *68*, 5020.
(23) Wyslouzil, B. E.; Seinfeld, J. H.; Flagan, R. C.; Okuyama, K. *J. Chem. Phys.* **1991**, *94*, 6842.
(24) Raes, F.; Saltelli, A.; van Dingenen, R. *J. Aerosol Sci.* **1992**, *23*, 337.
(25) Viisanen, Y.; Kulmala, M.; Laaksonen, A. *J. Chem. Phys.* **1997**, *107*, 920.
(26) Flood, H. *Z. Phys. Chem.* **1934**, *A170*, 286.
(27) Volmer, M.; Flood, H. *Z. Phys. Chem.* **1934**, *A119*, 277.
(28) Neumann, K.; Döring, W. *Z. Phys. Chem.* **1940**, *A186*, 203.
(29) Reiss, H. *J. Chem. Phys.* **1950**, *18*, 840.
(30) Binder, K.; Stauffer, D. *Adv. Phys.* **1976**, *25*, 343.
(31) Renninger, R. G.; Hiller, F. C.; Bone, R. C. *J. Chem. Phys.* **1981**, *73*, 1584.
(32) Trinkhaus, H. *Phys. Rev. B.* **1983**, *27*, 7372.
(33) Wilemski, G. *J. Chem. Phys.* **1984**, *80*, 1370.
(34) For a review, see: Mirabel, P. J.; Jaeker-Voirol, A. Binary Homogeneous Nucleation. *Lect. Notes Phys.* **1988**, *309*, 3.
(35) Wilemski, G.; Wyslouzil, B. E. *J. Chem. Phys.* **1995**, *103*, 1127.
(36) Kathmann, S. M.; Hale, B. N. *Proceedings of The 14th International Conference on Nucleation and Atmospheric Aerosols*; Nucleation and Atmospheric Aerosols; Kulmala, M., Wagner, P. E., Eds. Elsevier: Amsterdam, The Netherlands, 1996; p 30.
(37) Bennett, C. H. *J. Comput. Phys.* **1976**, *22*, 245.

(38) GAMESS Quantum Chemistry software; Ames Laboratory, Iowa State University: Ames, IA, **1993**.
(39) Stauffer, D. *J. Aerosol Sci.* **1976**, *7*, 319.
(40) Kremer, K. *J. Aerosol Sci.* **1977**, *9*, 243.
(41) Shi, G.; Seinfeld, J. H. *J. Chem. Phys.* **1990**, *93*, 9033.
(42) Nishioka, K.; Fujita, K. *J. Chem. Phys.* **1994**, *100*, 532.
(43) McGraw, R. *J. Chem. Phys.* **1995**, *102*, 2098.
(44) Shugard, J.; Reiss, H. *J. Chem. Phys.* **1976**, *65*, 2827.
(45) Wilemski, G. *J. Chem. Phys.* **1988**, *88*, 5134.
(46) Hale, B. N. *Phys. Rev. A* **1986**, *33*, 4156.
(47) Hale, B. N.; Wilemski, G. *Chem. Phys. Lett.* **1999**, *305*, 263.
(48) Hale, B. N.; Ward, R. *J. Stat. Phys.* **1982**, *28*, 487.
(49) Kemper, P. *A Monte Carlo Simulation of Water Clusters*, Ph.D. Thesis, University of Missouri—Rolla, Rolla, MO, 1990.
(50) Hale, B. N. *Aust. J. Phys.* **1996**, *49*, 425.
(51) Kubo, R. *Statistical Mechanics*; North-Holland-American Elsevier: New York, 1971; Chapter 3.
(52) McQuarrie, D. A. *Statistical Thermodynamics*; Harper Collins: New York, 1973.
(53) Metropolis, M.; Rosenbluth, A.; Rosenbluth, M.; Teller, A.; Teller, E. *J. Chem. Phys.* **1953**, *121*, 087.
(54) Arnold, F.; Fabian, R.; Joos, W. *Geophys. Res. Lett.* **1981**, *8* (3), 293.
(55) Arnold, F.; Fabian, R. *Nature* **1980**, *283*, 55.
(56) Yue, G. K.; Poole, L. R.; Wang, P. H.; Chiou, E. W. *J. Geo. Phys. Res.* **1994**, *99*, 3727.
(57) Lovas, F. J.; Kuczkowski, R. L.; Suenram, R. D. *J. Am. Chem. Soc.* **1981**, *103*, 2561.
(58) Kurdi, L.; Kochanski, E. *Chem. Phys. Lett.* **1989**, *158*, 111.
(59) Brciz, A.; Karpfen, A.; Lischka, H.; Schuster, P. *Chem. Phys.* **1984**, *89*, 337.
(60) Hofmann, M.; Von Rague Schleyer, P. *J. Am. Chem. Soc.* **1994**, *116*, 4947.
(61) Kuczkowski, R. L.; Suenram, R. D.; Lovas, F. J. *J. Am. Chem. Soc.* **1981**, *103*, 2561.
(62) Rahman, A.; Stillinger, F. H. *J. Chem. Phys.* **1978**, *68*, 666.
(63) Allen, M. P.; Tildesley, D. J. *Computer Simulation of Liquids*; Oxford University: Oxford, U.K., 1987.
(64) Weast, R. C. *CRC Handbook of Chemistry and Physics*, 65th ed.; CRC Press Inc.: Boca Raton, FL, 1989; D-266.
(65) Lee, J. K.; Barker, J. A.; Abraham, F. F. *J. Chem. Phys.* **1973**, *58*, 3166.
(66) Hale, B. N. Private communication.
(67) Hale, B. N.; DiMattio, D. J. *Nucleation and Atmospheric Aerosols 2000*, AIP Conference Proceedings; American Institute of Physics: Melville, NY, 2000; Vol. 534, p 31.
(68) Gmitro, J. I.; Vermeulen, T. *AIChE J.* **1964**, *10*, 740.
(69) Sabina, L.; Terpugow, L. *Z. Phys. Chem.* **1935**, *A173*, 237.
(70) Adamson, A. W. *Physical Chemistry of Surfaces*; John Wiley & Sons: New York, 1990; Chapter 3.
(71) Croxton, C. A. *Statistical Mechanics of the Liquid Surface*; John Wiley & Sons: New York, 1980; Chapter 1.